



Microstructure of commercial sheet out of Ti-6Al-4V alloy after superplastic forming at 700°C

M. R. Shagiev[†], M. A. Murzinova

[†]marat@imsp.ru

Institute for Metals Superplasticity Problems of the RAS, Ufa, 450001, Russia

The possibility of superplastic forming of commercial sheet out of Ti-6Al-4V alloy at rather low temperature $T=700^{\circ}\text{C}$ was shown for the first time in the present study. Experimental hemisphere with a radius of 35 mm was successfully formed at 700°C with a constant argon gas pressure $p=2.5$ MPa in 4352 seconds. Unlike to previous studies, preheating of the preform, superplastic forming process and subsequent cooling were carried out not in air but in vacuum, in order to avoid the formation of the surface oxide layer that limits the ductility resource of the material. Initial microstructure of Ti-6Al-4V alloy commercial sheet was found to be very non-homogeneous: along with ultrafine grains of α and β phases, the coarse elongated α grains with developed substructure were observed. After superplastic forming at 700°C a substantial improvement of microstructure homogeneity of the commercial sheet took place. Microstructure of the cross-section of the hemisphere did not contain coarse elongated grains. Although the average grain size remained almost unchanged ($d=1.4-1.5$ μm), the coefficient of variation decreased significantly, from 1.3 to 0.6. Microtexture analysis revealed randomization of the rolling texture in Ti-6Al-4V commercial sheet and decrease in the texture maximums after superplastic forming at 700°C .

Keywords: superplastic forming, Ti-6Al-4V titanium alloy, microstructure, texture.

1. Introduction

Technologies based on the superplasticity effect are of a great interest for manufacturing the complex-shaped products out of hard-to-deform materials [1,2]. For commercial ($\alpha+\beta$)-titanium alloys superplasticity can be achieved at high temperatures ($850-950^{\circ}\text{C}$) and low strain rates ($10^{-3}-10^{-4}$ s^{-1}) [1-3]. Under such deformation conditions, multiple slip develops not only in the β (body centered cubic lattice) phase but also in the α (hexagonal close-packed lattice) phase, grain boundary sliding and diffusion are facilitated [4]. At the same time deformation is accompanied by the development of processes of recrystallization and globularization of phases [5] that eliminates the non-homogeneity of the microstructure of commercial semi-finished products [6]. A homogeneous equiaxed microstructure with grain sizes of $d=5-10$ μm and close volume fractions of α and β phases, demonstrates high elongations and strain rate sensitivity [1,2,7]. However, high temperatures and low strain rates significantly retards the widespread application of superplastic technologies [1,2]. Superplasticity at low temperatures can be achieved either through the grain refinement to sizes less than $d<1$ μm [8-10] or through the development of alloys with

high content of β stabilizing elements [11]. So, Ti-6Al-4V titanium alloy with an ultrafine-grained structure exhibits high superplastic properties at $700-750^{\circ}\text{C}$ [8], while for commercial titanium alloys ($d\approx 5$ μm) this is the lower temperature range of superplasticity [1].

In the present work, the possibility of superplastic forming (SPF) of Ti-6Al-4V commercial sheet at $T=700^{\circ}\text{C}$ was demonstrated and the microstructure evolution in the superplastically formed specimen was analyzed.

2. Experimental

Commercial sheet out of VT6c (hereinafter referred to as Ti-6Al-4V) titanium alloy with thickness of 1 mm was used as a starting material. VT6c alloy is a modification of Russian VT6 alloy with reduced content of impurities, and its chemical composition complies with the Russian national standard GOST 19807-91 (Table 1).

The experimental technique of SPF of hemispheres with a radius of 35 mm and the design of special die tooling are given in [12,13]. Quasi-free forming in a cylindrical matrix was carried out at 700°C with a constant argon gas pressure $p=2.5$ MPa. Unlike [13], preheating of the die tooling and the SPF preform, the forming process and subsequent cooling

Table 1. Chemical composition of Ti-6Al-4V titanium alloy.

Element	Ti	Al	V	Zr	Fe	Si	O	C	N	H	Other impurities
Content, wt. %	base	5.3–6.5	3.5–4.5	≤ 0.3	≤ 0.25	≤ 0.15	≤ 0.15	≤ 0.1	≤ 0.04	≤ 0.015	≤ 0.3

were carried out in a vacuum, not in air, in order to avoid the formation of the surface oxide layer that limits the ductility resource of the material.

Mechanically polished microstructures of the cross-sections of both the commercial sheet and SPF hemisphere were analyzed using TESCAN MIRA 3 LMH FEG scanning electron microscope equipped with back-scattered electron (BSE) and electron backscatter diffraction (EBSD) detectors. EBSD analysis was performed with a step of 0.1 μm to obtain crystal orientation maps and with a step of 0.5 μm for microtexture studies. Different colors in the orientation maps correspond to certain crystal orientations; the color-code triangle is shown in the upper right corner of the maps. Boundaries with misorientations of more than 15° were considered as high angle boundaries and are shown as black lines in crystal orientation maps. Boundaries with misorientations from 2° to 15° were considered as low angle boundaries and are shown as white lines in the maps. Misorientations less than 2° were not taken into account during EBSD analysis. The equivalent diameter was taken as the grain size.

3. Results and Discussion

Typical BSE image of microstructure and crystal orientation map of the cross-section of the Ti-6Al-4V sheet are shown in Figs. 1a and b, respectively. Initial microstructure of the commercial sheet was found to be very non-homogeneous: along with ultrafine α and β grains ($d < 1 \mu\text{m}$), the coarse elongated α grains with $d > 10 \mu\text{m}$ and developed substructure were observed (Fig. 1b). Aspect ratio of the α and β grains reached 9 and 5, respectively. Fraction of low angle boundaries exceeded 70%. Volume fraction of the β phase in the sheet was about 7%, however, according to [15], at the SPF temperature (700°C) it should be 15–20%.

Distribution of the grains of α and β phases by size in the sheet is given in Fig. 1c. The grain size varied from 0.3 to $25 \mu\text{m}$ in the α phase, and from 0.3 to $3 \mu\text{m}$ in the β phase. At the average grain size $d_{\text{sheet}} = 1.4 \mu\text{m}$ the coefficient of variation was $k_{\text{sheet}} = 1.3$.

Microtexture analysis of the commercial sheet revealed a rolling texture typical for titanium alloys thermomechanically processed in the $(\alpha+\beta)$ -phase region [14,16]: rather strong

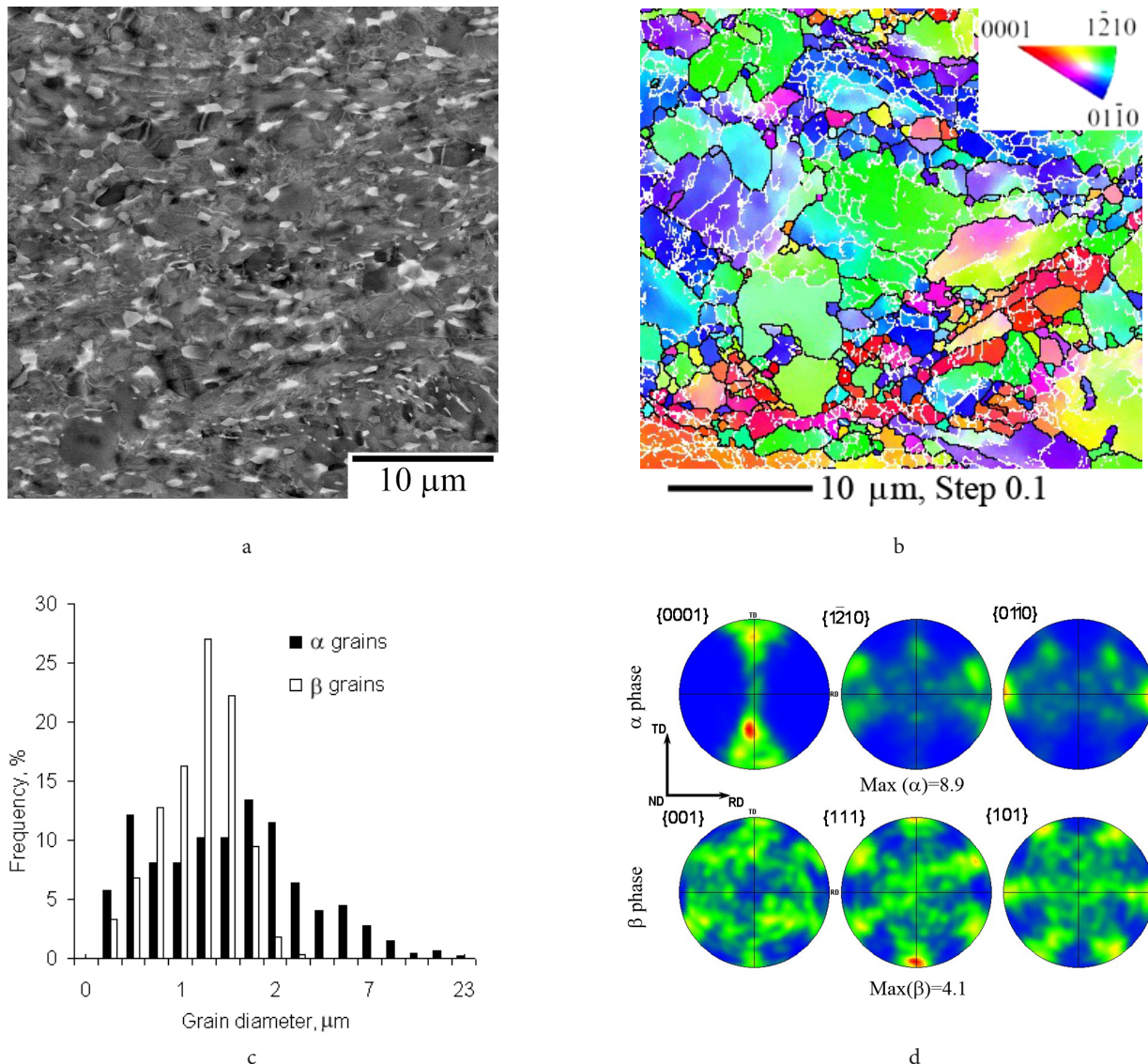


Fig. 1. (Color online) Typical BSE image of microstructure (a), crystal orientation map (b), distribution of grains by size (c), and microtexture (d) of the Ti-6Al-4V commercial sheet.

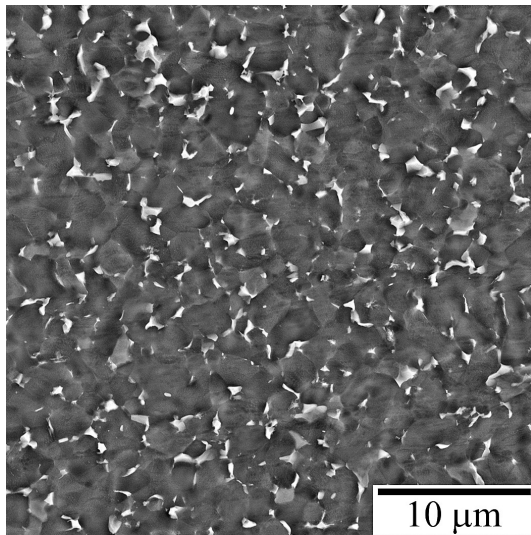
texture in the α phase and a weaker texture in the β phase (Fig. 1d). There were two maximums in the (0001) pole figure, which were tilted 20–40° from ND towards \pm RD. (Fig. 1c).

Experimental SPF hemisphere was formed at 700°C with constant argon gas pressure $p=2.5$ MPa in 4352 seconds (Fig. 2). Its surface was smooth, with no signs of oxidation. The thickness of the hemisphere gradually decreased from the edge ($h_{\text{edge}}=0.8$ mm) to the top ($h_{\text{top}}=0.3$ mm).

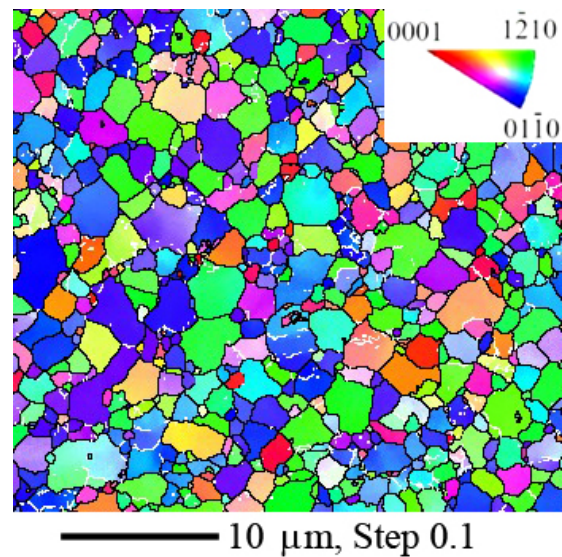
After SPF at 700°C, microstructure in the top of the hemisphere became more homogeneous and equiaxed (Figs. 3a,b). No coarse elongated grains were observed. Results of quantitative microstructural analysis also testify the improvement of the microstructure homogeneity (Fig. 3c). The grain size did not exceed 7 μm both in α and β phases, the aspect ratio was about 2. Despite the average grain size remained almost the same ($d_{\text{SPF}}=1.5$ μm), the coefficient of variation decreased considerably ($k_{\text{SPF}}=0.6$). The fraction of low angle boundaries after SPF also decreased to 15%.



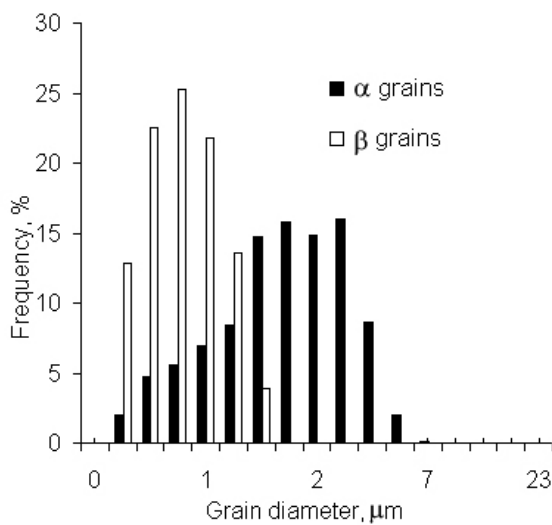
Fig. 2. Experimental SPF hemisphere.



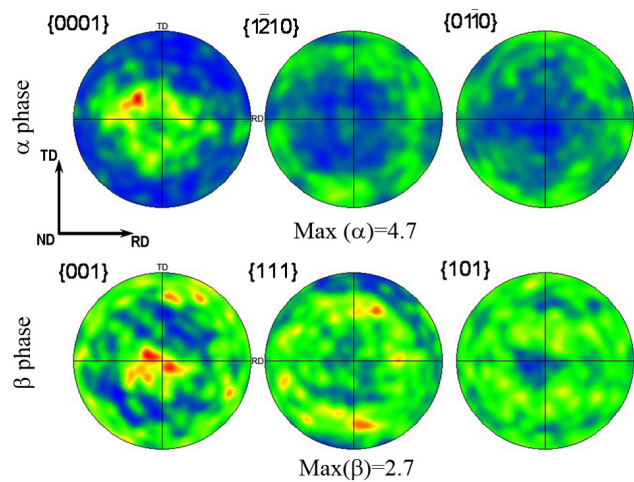
a



b



c



d

Fig. 3. (Color online) Typical BSE image of microstructure (a), crystal orientation map (b), distribution of grains by size (c), and microtexture (d) of the experimental SPF hemisphere.

Microtextures of material after SPF at 700°C are shown in Fig. 3d. Compared to microtextures of the sheet (Fig. 1d), they are more randomized and have lower intensities of texture maximums.

Unlike to high-temperature superplastic deformation, which can be accompanied by discontinuous recrystallization and globularization, during low-temperature superplastic deformation the processes of continuous recrystallization and recovery prevail [4]. On the other hand, in Ti-6Al-4V alloy with initial ultrafine-grained structure a slight increase in the grain size was observed at low strain rates [10]. The occurrence of these processes during SPF of Ti-6Al-4V commercial sheet at 700°C provided an increase in the microstructure homogeneity.

4. Conclusions

Superplastic forming of Ti-6Al-4V commercial sheet with non-homogeneous initial microstructure ($d = 0.3 - 25 \mu\text{m}$) at rather low temperature of 700°C with a constant argon gas pressure of 2.5 MPa was performed for the first time.

Superplastic forming of Ti-6Al-4V sheet at 700°C led to an improvement of microstructure homogeneity and randomization of the rolling texture.

Acknowledgements. The work was performed using the facilities of shared services center "Structural and Physical-Mechanical Studies of Materials" within the state assignment of the Institute for Metals Superplasticity Problems of the Russian Academy of Sciences. The authors are grateful to Dr. A. A. Kruglov, O. A. Rudenko and S. N. Gerasimenko for technical assistance.

References

1. O.A. Kaibyshev. Superplasticity of Alloys, Intermetallides and Ceramics. Springer-Verlag, Berlin (1992) 317 p. [Crossref](#)
2. A. Barnes. Journal of Materials Engineering and Performance. 16, 440 (2007). [Crossref](#)
3. E. Alabort, D. Putman, R.C. Reed. Acta Materialia. 95, 428 (2015). [Crossref](#)
4. S.L. Semiatin, V. Seetharaman, I. Weiss. Materials Science and Engineering A. 243, 1 (1998). [Crossref](#)
5. S.L. Semiatin, V. Seetharaman, I. Weiss. Materials Science and Engineering A. 263, 257 (1999). [Crossref](#)
6. Th.R. Bieler, S.L. Semiatin. International Journal of Plasticity. 18, 1165 (2002). [Crossref](#)
7. M.L. Meier, D.R. Lesuer, A.K. Mukherjee. Materials Science and Engineering A. 136, 71 (1991). [Crossref](#)
8. G.A. Salishchev, R.M. Galeev, O.R. Valiakhmetov, R.V. Safiullin, R.Ya. Lutfullin, O.N. Senkov, F.H. Froes, O.A. Kaibyshev. Journal of Materials Processing Technology. 116, 265 (2001). [Crossref](#)
9. P.N. Comley. Materials Science Forum. 447–448, 233 (2004). [Crossref](#)
10. S.V. Zharebtsov, E.A. Kudryavtsev, G.A. Salishchev, B.B. Straumal, S.L. Semiatin. Acta Materialia. 121, 152 (2016). [Crossref](#)
11. E. Alabort, D. Barba, M.R. Shagiev, M.A. Murzinova, R.M. Galeev, O.R. Valiakhmetov, A.F. Aletdinov, R.C. Reed. Acta Materialia. 178, 275 (2019). [Crossref](#)
12. F.U. Enikeev, A.A. Kruglov. International Journal of Mechanical Sciences. 37 (5), 473 (1995). [Crossref](#)
13. O.A. Rudenko, A.A. Kruglov, R.V. Safiullin, O.R. Valiakhmetov, R.Ya. Lutfullin. Forging and Stamping Production. Material Working by Pressure. 4, 5 (2006). (in Russian)
14. Q. Chao, P.D. Hodgson, H. Beladi. Materials Science and Engineering A. 694, 13 (2017). [Crossref](#)
15. N. Saunders. In: Titanium'95: Science and Technology (Eds. P. Bleckinsop, W.J. Evans, H.M. Flower). Institute of Materials, London (1996) 2167 p.
16. J. Fan, J. Li, Y. Zhang, H. Kou, L. Germain, C. Esling. Materials Characterization. 130, 149 (2017). [Crossref](#)